Catalysis Today 155 (2010) 311–318

Contents lists available at ScienceDirect

Catalysis Today

journal homepage: www.elsevier.com/locate/cattod

Electrical conductivity of a MoVTeNbO catalyst in propene oxidation measured in operando conditions

M. Caldararu [a,*], M. Scurtu [a], C. Hornoiu [a], C. Munteanu [a], T. Blasco [b,**], J.M. López Nieto [b]

[a] Institute of Physical Chemistry "Ilie Murgulescu" of the Romanian Academy, Spl. Independentei 202, 060021 Bucharest, Romania
[b] Instituto de Tecnología Química, UPV-CSIC, Campus Universidad Politécnica de Valencia, Avda. Los Naranjos s/n, 46022 Valencia, Spain

ARTICLE INFO

Article history:
Available online 1 March 2010

Keywords:
Electrical conductivity
MoVTeNb-phase
Propene oxidation
Acrylic acid
Surface reduction/oxidation
Effect of moisture

ABSTRACT

A complex ac electrical conductivity study was performed on a $Te_{0.33}MO_{3.33}$ (M = Mo + V + Nb) pure phase (M2-type phase) in operando conditions, using the differential step technique (DST). The aim is to obtain new information about the influence of the oxidation and moisture on the catalytic behaviour of this phase in propene oxidation to acrylic acid. Three successive series of experiments were performed on the same batch of sample: (i) cycles of heating (up to 300, 350 and 400 °C, respectively)–cooling (to room temperature) in inert and in the catalytic test mixture, without intermediate oxidation; (ii) the same, but intercalating heating–cooling oxidation cycles (up to 300, 350 and 400 °C, respectively) before the corresponding catalytic test runs; and (iii) catalytic testing runs performed by heating up to 400 °C in the presence of pre-absorbed or co-adsorbed humidity. Based on the electrical conductivity results, it appears that 350 °C is a critical temperature in terms of surface reduction/re-oxidation: below this temperature no major surface changes of the relative oxidation level occur on flushing in dry helium or in the catalytic test mixture, while above it, an important reduction occurs in the same atmospheres. Re-oxidation in oxygen is not efficient if performed below 350 °C, but if done above (up to 400 °C) the surface recovers almost the initial behaviour. These results suggest the reversibility of the oxidation state of the catalyst surface, which is important in the practical use of this material. The activity and selectivity of acrylic acid formation are discussed in relation with the relative levels of oxidation/reduction of the surface.

1. Introduction

Mo–V–Te–Nb–O mixed metal oxides have been reported as efficient catalysts in the (amm)oxidation of propane to acrylonitrile [1,2] or to acrylic acid [3,4] and in the oxidative dehydrogenation (ODH) of ethane to ethylene [5,6]. Efficient catalysts consist of at least two main crystalline phases [2,4–13]: (i) an orthorhombic phase, i.e. $TeM_{20}O_{31}$ (the so-called M1-phase), isomorphous with $Cs_x(Nb,W)_5O_{14}$ [14]; and (ii) a pseudohexagonal or orthorhombically distorted phase, i.e. $Te_{0.33}MO_{3.33}$ (the so-called M2 phase), isomorphous with $K_{0.13-0.33}WO_3$ [15]. M1 is responsible for the selective alkane activation, while both M1 and M2 phases are effective in propene (amm)oxidation [5–13]. Moreover, phase cooperation between M1 and M2 seems to have a positive influence on the selectivity, particularly when working at high propane conversions [10,16,17].

M1 and M2 structures can be described as corner sharing MO_6 (M = Mo, V, Nb) octahedra networks forming 5-, 6- and 7-member-ring channels in M1, and 6-member-ring channels in phase M2, with tellurium occupying cationic sites in the hexagonal channels (TeO_3E and TeO_4E, respectively) [6–13]. M1 phase has V^{5+} centers, while all vanadium is present as V^{4+} in M2-phase, which could explain the inability of the latter for alkane activation [10,13]. The chemical composition of the M2-phase influences its catalytic behaviour [18–20], especially in propene oxidation [18]: Nb-free M2 oxide is selective in the oxidation to acrolein, while the Nb-containing one is selective in the oxidation to acrylic acid.

Most papers report about the necessity of final calcination of the precursors under inert (N_2 or Ar) atmosphere, in order to avoid phase segregation of the components and surface oxidation [21,22]. It was claimed that a high excess of gas phase oxygen supplied during testing leads to over-oxidation of surface molybdenum and waste formation; however, sufficient oxygen should be fed in order to prevent excessive reduction of the surface.

Surface oxidation or reduction of the semiconductor oxides used in catalysis can be investigated by following the evolution of the electrical properties of the solid in relation with a specific atmosphere. Exposure to oxygen of an *n*-type oxide leads to the

* Corresponding author. Tel.: +40 213121147; fax: +40 213121147.
** Corresponding author. Tel.: +34 963877812; fax: +34 963877809.
E-mail addresses: mcaldararu@chimfiz.icf.ro (M. Caldararu), tblasco@itq.upv.es (T. Blasco).

0920-5861/$ – see front matter © 2010 Elsevier B.V. All rights reserved.
doi:10.1016/j.cattod.2010.01.045

decrease of conductivity with respect to that in inert atmosphere, as a result of oxygen ion adsorption as follows:

$$O_{2(gas)} + e \leftrightarrow O_2^- + e \leftrightarrow 2O^- \quad (1)$$

the electrons trapped by the adsorbed oxygen being provided by the surface of the oxide. On the contrary, flushing with helium facilitates either desorption of pre-adsorbed oxygen ions or even formation of anion vacancies by lattice oxygen migration at high temperature. The interaction with a reducing gas such as hydrocarbon (propene) results either in formation of anion vacancies V_O (Mars van Krevelan mechanism) acting as electron donors:

$$O_{(lattice)} + \text{hydrocarbon} \rightarrow \text{oxidation products} + V_O \quad (2)$$

or in the consumption of the oxygen ad-ions. Both variants result in the increase of electron carrier concentration and thus in the increase of conductivity. The partial oxidation products (if any) can act also as reducing compounds during their contact with the catalyst surface.

Polycrystalline oxides (powders) may be modeled by a network consisting of highly conducting grains separated by poorly conducting inter-grain contacts [23]. This network can be correspondingly represented by a series of parallel *R–C* (resistance–capacitance) circuits, assimilated with an equivalent parallel R_p–C_p frequency dependent circuit, the simplest possible circuit having a physical analog. Studies of the resistance dispersion with frequency indicated two frequency independent regions—one where the measured value of the effective resistance ($R = 1/G$, where G is conductance) is represented (in a simplified manner) by the sum of grain and inter-grain (contact) resistances (R_s and R_c, respectively), and the other one, at very high frequencies, where the measured value is controlled only by grain (bulk) resistance. As will be presented further, in the case of the experiments presented here (non-sintered, non-pressed powder) the measured effective resistance (conductance) is dominated by Schottky-type barriers developed in inter-grain areas [24]; the height of these barriers is influenced by changes in composition, charge, coverage and dielectric constant (ε) of the surface layer in inter-grain areas [25]. Surface reduction or oxidation, hydration/dehydration and/or adsorption/desorption/reaction are mainly reflected in the topography of inter-grain areas, and will also modify the dielectric constant of the surface layer (thus the height of the inter-grain barriers), as a result of the modification on the nature and mobility of the surface dipoles [26]. Thus, by combined effect of atmosphere on the grain surface and on the inter-grain barrier heights, it is possible to follow the dynamics of gas–surface interactions, by monitoring the changes in the relative oxidation levels of the catalysts surfaces under reaction conditions [27–29].

In this paper, we studied *in operando conditions*, the changes of the electrical conductivity σ of a Mo–V–Te–Nb–O model catalyst (M2-type phase, active and selective in propene oxidation to acrylic acid) under various atmospheres between 20 and 400 °C, using the differential step technique (DST) [27–29]. Since the simultaneous effects of the temperature and atmosphere make the interpretation of conductivity data very complex, we have used this technique in order to be able to separate them. DST consists of successive heating–cooling cycles performed on the same sample in various atmospheres, according to a certain protocol. The conductivity data are commented by comparing the plots of a specific cycle, with those obtained in the previous or in the next one. If thermal cycling is performed in identical conditions and between the same temperature limits, the differences between plots at a certain temperature indicate just the specific effect of a certain atmosphere. Thus, using this technique one can obtain valuable information on the evolution of the catalyst surface under reaction conditions, e.g. on the surface dynamics in terms of its relative oxidation level. The primary goal of this study was to follow only the phenomenological aspects and not to obtain absolute values of conductivity/activity.

2. Experimental

2.1. Catalyst preparation

The catalyst named as MoVTeNb-M2 with a final Mo/V/Te/Nb atomic ratio of 0.78/0.3/0.39/0.12 was prepared from an aqueous slurry of the corresponding salts as reported elsewhere [18] and calcined at 600 °C for 2 h in N_2 flow.

2.2. Catalyst characterization

X-ray diffraction patterns (XRD) were collected using a Philips X'Pert diffractometer equipped with a graphite monochromator, operating at 40 kV and 45 mA and employing nickel-filtered CuK_α radiation ($\lambda = 0.1542$ nm). Scanning electron microscopy (SEM) and EDX microanalyses were performed on a JEOL JSM 6300 LINK ISIS instrument. The quantitative EDX analysis was performed using an Oxford LINK ISIS System with the SEMQUANT program, which introduces the ZAF correction.

2.3. Operando electrical conductivity

The electrical conductivity measurements were performed on the catalyst powder, under *operando* conditions, i.e. in gas flow, using the differential step technique (DST) and monitoring permanently the composition of the inlet/exit gas (on-line coupled GC) at atmospheric pressure [27–30].

A precision RLC Bridge (TESLA BM 484), measuring the admittance Y at 1592 Hz allowed to follow simultaneously the evolution of parallel conductance (G_p) and capacitance (C_p) of the specially designed conductivity cell filled with catalyst grains [28]. The cell consists of two coaxial tantalum cylinders (as electrodes) supported on a glass frit and embedded in a glass cell, with the bed of catalyst grains (1.4 cm^3, fraction between 0.25 and 0.5 mm) filling the annular space. The conductivity σ (S/m) was calculated from the corresponding G_p values by taking into account the special cylindrical geometry of the sample [30] (the height of the electrodes $H = 28$ mm, the height of the catalyst bed $h = 8.5$ mm, the radius of external electrode $r_{ext} = 8.1$ mm and of the internal one $r_{int} = 3.7$ mm).

The differential step technique (DST) applied in these measurements [27–30] consists in general of successive heating–cooling cycles performed on the same batch of powder in various gases according to a specific protocol: dry helium (**DHe**), dry oxygen (**DO**), humid oxygen (**HO**), and in the reaction mixture used for the catalytic test (**CT**) (i.e. in this case, propene–oxygen–He mixture with the molar ratio 2/8/90). The total flow rate was 63 cm^3/min. The peculiarities of surface interaction with a certain atmosphere (in conditions similar to those of the catalytic experiment) can be identified by comparing the pattern of the evolution of G_p (and of corresponding C_p) with temperature in a specific cycle with those obtained in the previous and in the next runs, respectively, and by correlating these changes with the composition of the exit gas (as for example the content of water in the exit gas in the case of sample dehydration, or of the products in the case of catalytic tests).

Specifically, in this paper, the sample was successively submitted to cycles of heating in a specific atmosphere, by progressively increasing the maximum temperature of the cycle (up to 300, 350 and 400 °C, respectively), followed by cooling at room temperature. Heating from room temperature up to the final

temperature was linear (2 °C/min); cooling was faster (~10 °C/min) in the same atmosphere. After cooling, the closing stopcock was turned out and the sample was kept (statically) overnight in the same atmosphere at room temperature. Before each new cycle the sample was flushed for 30 min at room temperature in the corresponding gas atmosphere. Thus, each cycle started from the room temperature and ended at the specified one. This is followed by cooling at room temperature. The next cycle starts with 30 min of room temperature flushing in the new atmosphere, etc.

The protocol of the experiments used here consisted of three successive series of cycles, **A** → **B** → **C** (performed without changing the powder) where **A**, **B**, **C** were as in the schemes:

(i) **A-series** (experiments performed without intermediate oxidation cycles):

DHe1$^{(300)}$ → **CT1**$^{(300)}$ → **DHe2**$^{(350)}$ → **CT2**$^{(350)}$ → **DHe3**$^{(400)}$ → **CT3**$^{(400)}$ → **DHe4**$^{(400)}$;

(ii) **B-series** (experiments performed with intermediate oxidation cycles):

DHe5$^{(120)}$ → **DO1**$^{(300)}$ → **CT4**$^{(300)}$ → **DHe6**$^{(350)}$ → **DO2**$^{(350)}$ → **CT5**$^{(350)}$ → **DHe7**$^{(400)}$ → **DO3**$^{(400)}$ → **CT6**$^{(400)}$;

(iii) **C-Series** (Experiments performed in the presence of water in the feed):

DO4$^{(400)}$ → **HO**$^{(400)}$ → **CT7**$^{(400)}$ → **HCT**$^{(400)}$

where **HCT** represents the humid mixture used in the catalytic test. The humid mixtures (**HO** and **HCT**) have been obtained by passing the gas flow over the water layer in a saturator. The numbering of each specific series of cycles (i.e. **DHe**, **DO** and **CT**) corresponds to the order of performing that type of cycle in the whole set (**A**–**C**) of experiments (i.e. for **DHe** from **1** to **7**, for **DO** from **1** to **4**, for **CT** from **1** to **7**). The figures in brackets (superscripts) indicate the maximum heating temperature for each cycle.

The analysis of the effluent was performed by GC (TCD detector), on two parallel columns (HAYSEP Q and molecular sieves 5A) by sampling periodically the gases during the linear heating in the conductivity measurements.

The catalytic activity data were calculated based on the carbon balance, using the product distribution obtained in **CT** runs

3. Results

Fig. 1 shows the XRD pattern of the calcined sample, which is characteristic of an M2 hexagonal type bronze (HTB) oxide phase [11,12], although the presence of $TeMo_5O_{16}$ as an impurity cannot be completely ruled out. The chemical composition of all catalyst crystals analyzed by X-ray microanalysis is $Te_{0.33}Mo_{0.70}(V/Nb)_{0.30}Ox$, with a V/Nb ratio of ca. 0.55, in good agreement to previous results on similar materials [11,12].

In order to investigate the influence of the feed composition on the oxidation level of the catalyst surface, and consequently on its catalytic behaviour, we studied simultaneously the electrical conductivity and the catalytic performance of the oxide surface in selective oxidation of propene.

Understanding conductivity data on oxides is not easy, since the thermal variation of the electrical conductivity is a complicated combination of several distinct temperature/atmosphere dependent variables. The total conductivity, σ, can be expressed in a very simplified manner by the relation $\sigma_t = \sigma_i + \sigma_e$, where σ_i represents ionic (cation or anion) conductivity, while σ_e represents electron (or hole) conductivity. It is usually considered that in the temperature ranges used in catalysis, the electronic conductivity prevails, due to the much higher mobility (in relation with much smaller size) of these carriers; consequently, with very few exceptions, the conductivity results in this field are discussed mainly in terms of electron/hole transfer. However, Brønsted acidity is directly related with proton conduction and in some circumstances, particularly for surface conductivity, it must be taken into account since proton mobility/conduction can prevail at low temperature in the presence of moisture.

As mentioned in Section 1, the model of Koops [23] was considered by various authors using ac conductivity measurements for catalytic materials [31–34]. Data were interpreted [31] as corresponding to the grain controlled effective resistance, while others [32–34] considered the combination of grain and contact resistances. Based on literature data and on our measurements at the frequency used here [35], we considered also the last variant for which G_p can be reduced to $G_p = G_c G_s/(G_c + G_s)$ (with $G_c = 1/R_c$, where R_c is the contact resistance, and $G_s = 1/R_s$ is the bulk conductance). Since in the peculiar conditions of the experiment (a bad contact between non-sintered non-pressed grains) it can be considered that $G_s \gg G_c$, it follows that $G_p \sim G_c$, thus in agreement with the model of Schottky barrier controlled conductivity [24]. This model is supported also by the fast response of the conductivity values on changing the gaseous atmosphere.

3.1. Experiments performed without intermediate oxidation cycles (A-series)

Preliminary experiments on the MoVTeNbO catalyst submitted to successive cycles in dry helium (not presented here) showed a progressive conductivity increase, reflecting the enhancement of the number of charge carriers (electrons) by slight surface reduction on inert flushing. This indicates that the conductivity at high temperature is of *n*-type. However, as shown in Fig. 2(a–c), the increase of σ at low temperature proves the interference of proton conduction facilitated by the presence of weakly adsorbed water molecules, acting as "proton vehicles" [29,36,37]. Such an effect is frequently found for oxide powders [28,30], even in "dry" gases, due to the presence of very small traces of moisture in atmosphere (lost on heating, re-adsorbed on cooling). Indeed, heating at low temperature firstly increases the mobility of the weakly adsorbed molecular water species ("proton vehicles"), this enhancing the conductivity. Heating at slightly higher temperatures promotes desorption of weakly adsorbed water (which is detected in the effluent) this diminishing the contribution of proton conductivity. As a result, either a decreasing arm, or a peak appears in the low temperature region of the plot of the conductivity (σ) dependence with the temperature.

Fig. 2(a–c) shows the Arrhenius plots for the evolution of the catalyst conductivity with temperature in successive heating–cooling cycles in **A**-series under dry inert atmosphere (**DHe**) and under the corresponding test reaction mixture (**CT**). The plot for **DHe1**$^{(300)}$ run displays a peak with maximum at approximately 180 °C ($1000/T(K) = 2.2\ K^{-1}$) associated with water desorption

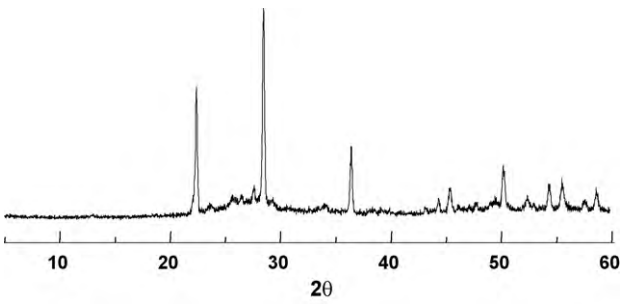

Fig. 1. XRD pattern of MoVTeNb-M2 catalyst.

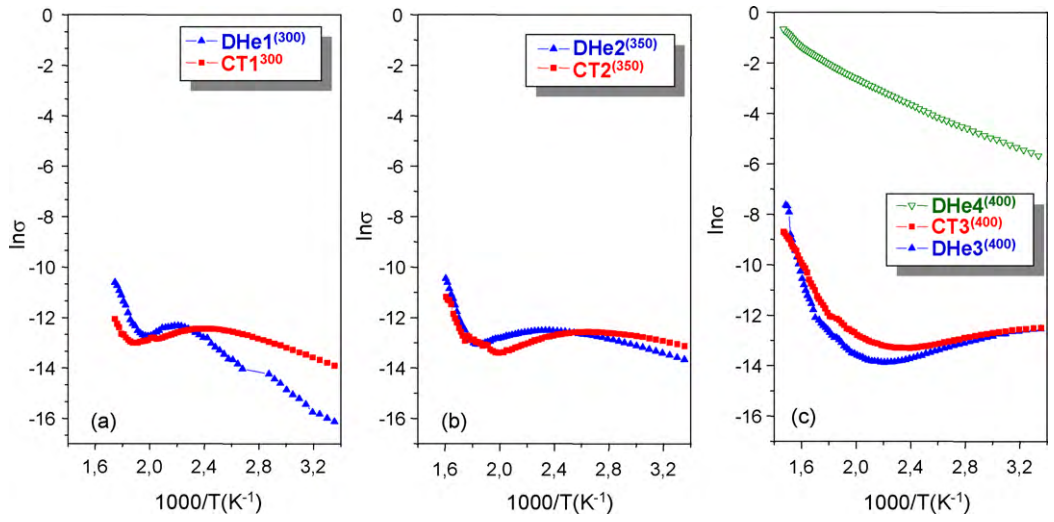

Fig. 2. Arrhenius plots for the variation of conductivity σ (S/m) on progressive heating of the MoVTeNb-M2 sample in **A**-series of experiments: (a) **DHe1**$^{(300)}$ and **CT1**$^{(300)}$; (b) **DHe2**$^{(350)}$ and **CT2**$^{(350)}$; (c) **DHe**3$^{(400)}$, **CT3**$^{(400)}$ and **DHe4**$^{(400)}$.

from the surface (see above), and a sharp increase of σ above 230 °C (1000/T(K) = 1.99 K^{-1}) indicating the increase of the lattice mobility, thus of its reducibility (Fig. 2a). Similar Arrhenius plots were also found for **CT1**$^{(300)}$ (Fig. 2a), **DHe2**$^{(350)}$ and **CT2**$^{(350)}$ runs (Fig. 2b), with the peak maxima slightly shifted to lower temperatures for **CT** runs.

The shape of the plots obtained for **DHe3**$^{(400)}$ and **CT3**$^{(400)}$ runs (Fig. 2c) is slightly different, with the minimum at around 180 °C (1000/T(K) = 2.2 K^{-1}); this indicates the shift of the temperature of the onset of lattice mobilization to lower values.

Attentive inspection of **DHe3**$^{(400)}$ run in Fig. 2c shows also a new sharp increase in conductivity (and thus in the level of surface reduction) above 385 °C (1000/T = 1.52 K^{-1}). However, no obvious σ enhancement was observed in the next **CT3**$^{(400)}$ run at low temperature (as it would have been expected for a partially reduced surface), probably because of the presence of oxygen in the feed. The most relevant result reported in Fig. 2c is the dramatic increase of σ in the next **DHe4**$^{(400)}$ run, indicating the reduction of the catalyst surface at high temperature in the previous run, i.e. in **CT3**$^{(400)}$. Since no significant conductivity enhancement was observed in **DHe3**$^{(400)}$ run (measured after the catalytic test up to 350 °C, run **CT2**$^{(350)}$, see the protocol), it means that major changes occurred by treating the catalyst with the reaction mixture in the temperature range 350–400 °C, possibly associated with much higher lattice mobilization above 350 °C. The simultaneous analysis of the effluent in **DHe4**$^{(400)}$ cycle showed large amounts of water evolved on heating up to 180 °C, which may also contribute to the very high conductivity values. Also traces of CO_2 and other products were detected in effluent above 240 °C; we suppose that they are probably resulting from the decomposition of some strongly bonded carbonate/carboxylate surface species formed by cooling the reduced surface in CT mixture (see the protocol).

Fig. 3 shows the variation of the propene conversion (left) and selectivity to acrylic acid (right) with reaction temperature during the catalytic tests in **A**-series (**CT1**$^{(300)}$, **CT2**$^{(350)}$ and **CT3**$^{(400)}$). During these experiments (performed without intermediate oxidation cycles) the highest conversion was obtained in **CT2**$^{(350)}$ run at 350 °C and was relatively high in the temperature range 340–400 °C in **CT3**$^{(400)}$ run giving a maximum at 380 °C.

Fig. 3 (right) displays the variation of the selectivity to acrylic acid for the same series of experiments. The best selectivity to acrylic acid (90–95%) was obtained at 320 °C in **CT2**$^{(350)}$ and above 350 °C in **CT3**$^{(400)}$. However, up to a temperature of 350 °C, the

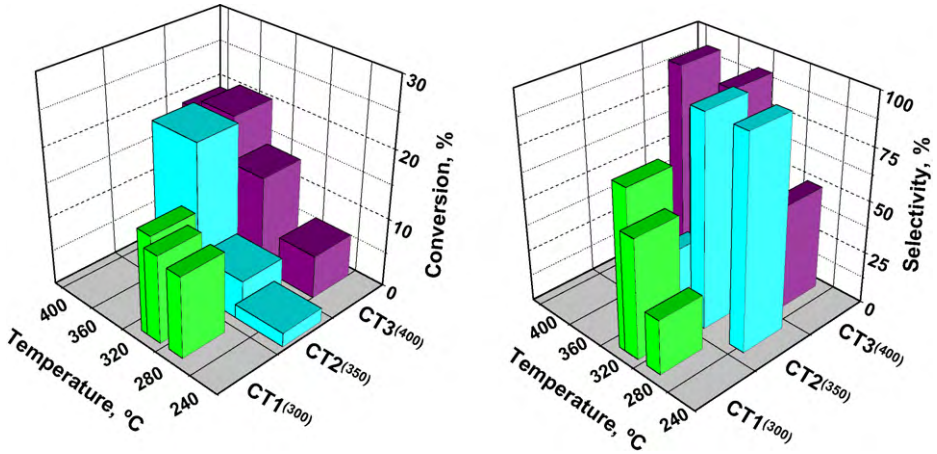

Fig. 3. Variation of propene conversion (left) and selectivity to acrylic acid (right) with the reaction temperature during various testing cycles of **A**-series: **CT1**$^{(300)}$; **CT2**$^{(350)}$; **CT3**$^{(400)}$. The catalytic experiments were carried out according to **A**-series (performed without intermediate oxidation cycles): **DHe1**$^{(300)}$ → **CT1**$^{(300)}$ → **DHe2**$^{(350)}$ → **CT2**$^{(350)}$ → **DHe3**$^{(400)}$ → **CT3**$^{(400)}$ → **DHe4**$^{(400)}$.

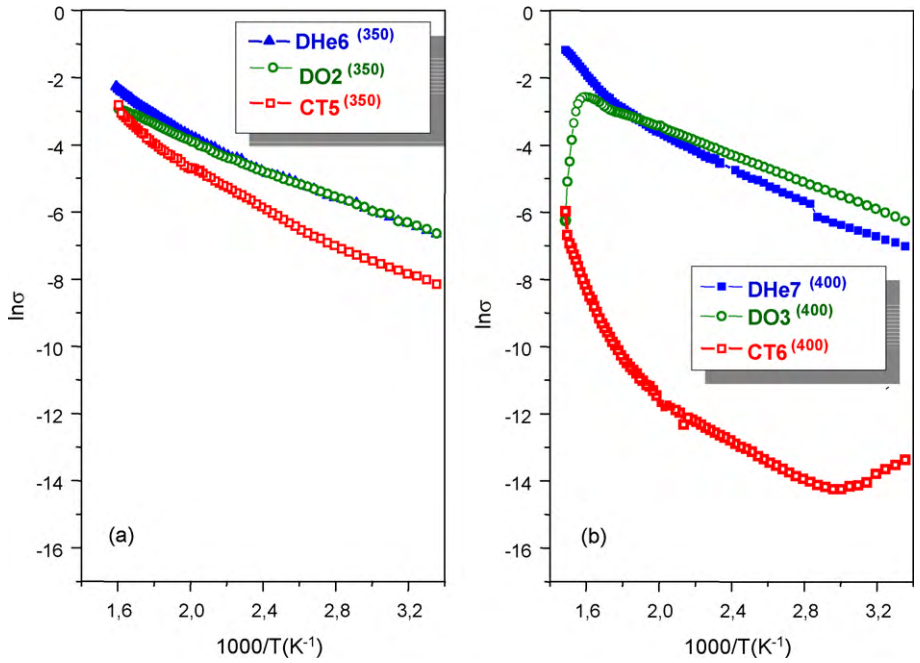

Fig. 4. Arrhenius plots for variation of conductivity σ (S/m) on progressive heating of the MoVTeNb-M2 sample in **B**-series of experiments (see the protocol). (a) **He6**$^{(350)}$, **DO2**$^{(350)}$ and **CT5**$^{(350)}$; (b) **DHe7**$^{(400)}$, **DO3**$^{(400)}$ and **CT6**$^{(400)}$.

selectivity to acrylic acid is lower for **CT3**$^{(400)}$ (Fig. 3, right), pointing out that it decreases as the extent of the catalyst reduction (as shown by the conductivity plots) increases.

3.2. Experiments performed with intermediate oxidation cycles (B-series)

The same portion of sample used in **A**-series of experiments, with the surface highly reduced as shown by the **DHe4**$^{(400)}$ plot in Fig. 2c, was submitted to **B**-series of experiments in order to investigate the effect of the additional surface oxidation on the catalyst performances. The evolution of conductivity (used to follow the change in the relative oxidation levels) is presented in Fig. 4.

After **DHe4**$^{(400)}$ run and subsequent cooling and re-heating in dry helium up to 120 °C (**DHe5**$^{(120)}$, not shown), the catalyst was re-heated under oxygen flow (**DO1**$^{(300)}$, not shown) and in the reaction mixture up to 300 °C (**CT4**$^{(300)}$, not shown). For the sake of simplicity these conductivity results were not presented here; however it should be mentioned that even if the evolution of conductivity during the last two cycles showed progressive surface oxidation (see for comparison **DHe4**$^{(400)}$ in Fig. 2c and **DHe6**$^{(350)}$ in Fig. 4a), σ values still remained very high with respect to the fresh sample (**DHe1** cycle); this indicates that only partial re-oxidation of the surface occurred on heating the solid up to 300 °C. Only small amounts of water but no oxidation products were detected in the effluents in **DHe5**$^{(120)}$ and **DO1**$^{(300)}$ runs, indicating that the catalyst surface has been effectively cleaned of the hydrocarbon residues formed in **DHe4**$^{(400)}$.

The Arrhenius plots of the conductivity vs. temperature for runs performed with heating up to 350 °C (**DHe6**$^{(350)}$, **DO2**$^{(350)}$ and **CT5**$^{(350)}$) and 400 °C (**DHe7**$^{(400)}$, **DO3**$^{(400)}$ and **CT6**$^{(400)}$) are shown in Fig. 4a and b, respectively. Although the conductivity remains still high during **DO2**$^{(350)}$, the slightly lower σ values measured at room temperature during next flushing and subsequent heating in **CT5**$^{(350)}$ run indicate that some surface oxidation occurred on heating in oxygen flow up to 350 °C, and subsequent cooling. This slight oxidation is not very stable, since the oxide surface turns to a more reduced state by performing the catalytic test up to 350 °C (**CT5**$^{(350)}$) (see the plot of the subsequent **DHe7**$^{(400)}$ run in Fig. 4b). However, the conductivity decreases dramatically between 350 and 400 °C during oxidation of the M2-type sample in **DO3**$^{(400)}$ run. The sharp decrease above 355 °C ($1000/T(\mathrm{K}) = 1.59\ \mathrm{K}^{-1}$) clearly indicates sudden surface oxidation, a statement also supported by the much lower conductivity values in **CT6**$^{(400)}$ run (Fig. 4b). At the same time, on re-heating in the catalytic test mixture up to 400 °C, σ progressively increases with temperature, this indicating again surface reduction **CT6**$^{(400)}$.

Please note that the effect of a specific treatment on the surface properties occurs mainly at the highest temperature of that cycle, and possibly on cooling down the sample in the same atmosphere. Accordingly, the effect of a certain treatment on conductivity appears more obvious at the beginning of the next cycle. For example, the plot of **DO2**$^{(350)}$ run is only slightly lower than that of **DHe6**$^{(350)}$, thus higher than that of the next **CT5**$^{(350)}$ one (instead of being lower, as would have been expected for an *n*-type semiconductor) (Fig. 4a). However, **CT5**$^{(350)}$ plot started at lower values, since it occurred on a surface previously oxidized. In the same sense, the conductivity measured in **CT6**$^{(400)}$ is much lower than in **DO3**$^{(400)}$ (Fig. 4b), because the latter started with the catalyst surface reduced after the catalytic test up to 350 °C (**CT5**$^{(350)}$).

Fig. 5 shows the propene conversion (left) and the selectivity to acrylic acid (right) with the reaction temperature during propene oxidation on the catalyst submitted to different oxidation cycles, i.e. in **CT5**$^{(350)}$ and **CT6**$^{(400)}$ runs (in **B**-series). For comparison the results achieved during the **C**-series of cycles (i.e. **CT7**$^{(400)}$ and **HCT**$^{(400)}$) are also included and will be discussed latter. The propene conversion increases as the temperature of the catalyst re-oxidation increases from 350 to 400 °C, indicating an increase in the number of the effective active sites from experiments **CT5**$^{(350)}$ to **CT6**$^{(400)}$. The propene conversions achieved during these experiments were lower than those of **A**-series (Fig. 3), which also indicates that the catalysts surface is not completely restored after being submitted to these re-oxidation cycles.

3.3. Experiments performed in the presence of water in the feed (C-series)

Series-C of experiments started with heating the M2 phase with dry oxygen up to 400 °C (experiment **DO4**$^{(400)}$) in order to clean the surface of possibly existing carbonaceous residues, and then the experiments were carried out on the oxidized catalyst. The effect of water on the catalyst surface conductivity was studied by measuring it under the following conditions: (i) heating–cooling in humid oxygen flow (run **HO**$^{(400)}$); (ii) flushing the reaction mixture over this pre-humidified surface (**CT7**$^{(400)}$); (iii) flushing humid reaction mixture (**HCT**$^{(400)}$).

As discussed above, the oxide surface is highly reduced at the end of the **CT6**$^{(400)}$ cycle and then the plot of the next cycle (**DO4**$^{(400)}$) starts from rather high σ values in the low temperature range, but the next **HO** run displays lower values (Fig. 6).

The conductivity at low temperature in **HO**$^{(400)}$ run results from the combination of two opposite effects: a conductivity decrease up to 75 °C, due to the desorption of proton vehicles (i.e. weakly adsorbed water species pre-adsorbed during 30 min flushing at room temperature [26,27,30]), while above this temperature, oxygen adsorption and surface oxidation prevail.

The conductivity plot of the subsequent experiment **CT7**$^{(400)}$, performed on the catalyst with pre-adsorbed water and oxygen on its surface (also as a result of cooling in humid oxygen) is very similar to that of **CT6**$^{(400)}$ carried out on the dry surface. However, in experiment **HCT**$^{(400)}$, in which water is fed with the reaction mixture, the conductivity is higher than in similar **CT** cycles (Fig. 6), indicating that the effect of moisture is more important when it is fed with the reaction mixture rather than separately with oxygen.

To summarize, the results shown in Figs. 4b and 6 indicate that:

(i) The gaseous oxygen oxidizes the M2-type phase surface mainly at high temperature (above 355 °C), diminishing the electronic conductivity, which is also supported by the lower conductivity values in the subsequent **CT6**$^{(400)}$ experiment. The conductivity remains low even in the presence of moisture (in experiment **HO**$^{(400)}$) and on testing the pre-humidified surface (**CT7**$^{(400)}$ experiment).

(ii) The presence of moisture in the hydrocarbon–oxygen mixture fed on the pre-reduced oxide increases the surface conductivity. This can be tentatively explained by assuming that the anion vacancies are partly filled with adsorbed water instead of oxygen during the low (room) temperature flushing sequence. Part of these water species desorbs on heating, and another part is chemisorbed on further heating, inhibiting extensive surface oxidation.

(iii) The initial oxidation state of the oxide (with the surface partially reduced by heating under the reaction mixture up to 400 °C) is recovered only by repeated heating in the presence of oxygen (including **HO** run) (compare plots for **CT3**$^{(400)}$, **CT6**$^{(400)}$ and **CT7**$^{(400)}$ runs).

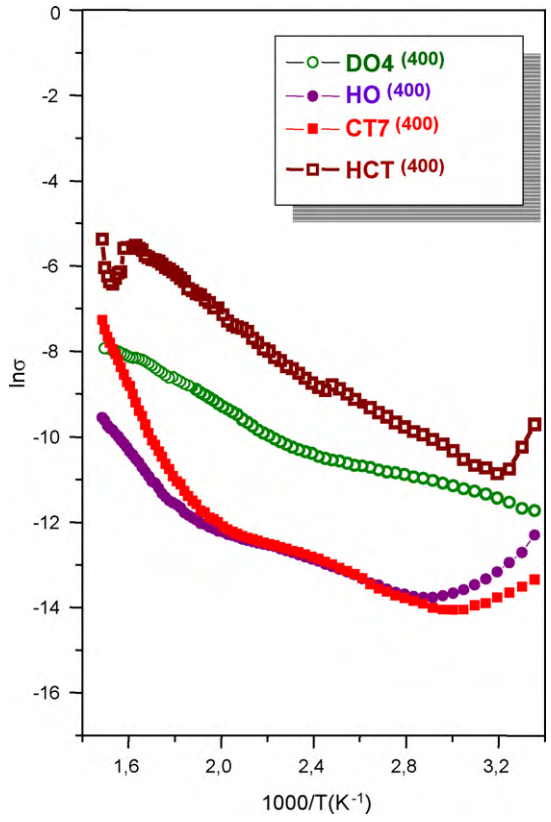

Fig. 6. Arrhenius plots for variation of conductivity σ (S/m) on progressive heating of the MoVTeNb-M2 sample in **C**-series of experiments: **DO4**$^{(400)}$, **HO**$^{(400)}$, **CT7**$^{(400)}$, **HCT**$^{(400)}$.

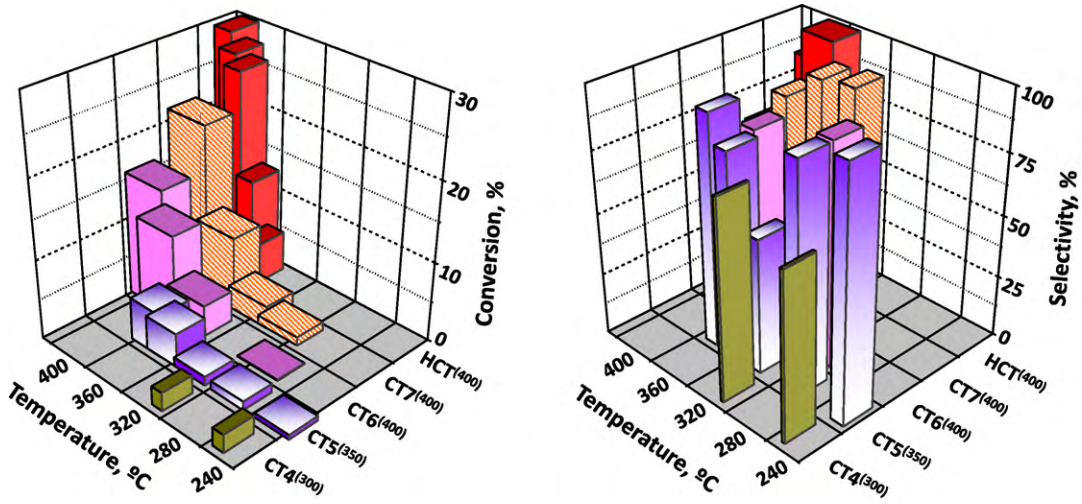

Fig. 5. Variation of propene conversion (left) and selectivity to acrylic acid (right) with the reaction temperature during various testing cycles: **CT5**$^{(350)}$; **CT6**$^{(400)}$; **CT7**$^{(400)}$; **HCT**$^{(400)}$. For comparison, the catalytic results achieved during the **CT4**$^{(300)}$ cycle are also included. The catalytic experiments were carried according to the **B**-series (experiments performed with intermediate oxidation cycles): **DHe5**$^{(120)}$ → **DO1**$^{(300)}$ → **CT4**$^{(300)}$ → **DHe6**$^{(350)}$ → **DO2**$^{(350)}$ → **CT5**$^{(350)}$ → **DHe7**$^{(400)}$ → **DO3**$^{(400)}$ → **CT6**$^{(400)}$ and **C**-series (experiments performed in the presence of water in the feed): **DO4**$^{(400)}$ → **HO**$^{(400)}$ → **CT7**$^{(400)}$ → **HCT**$^{(400)}$.

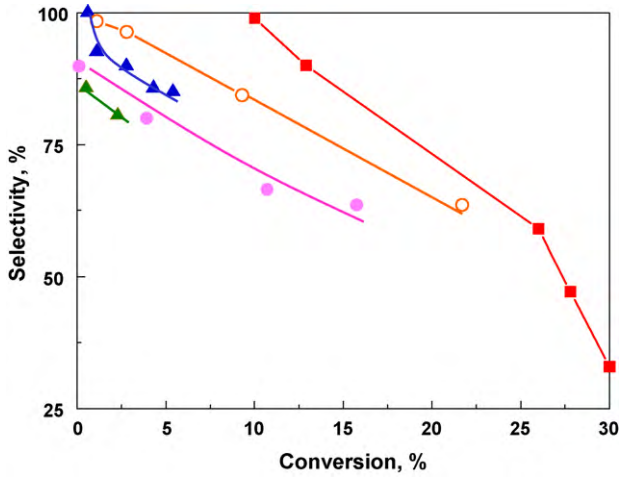

Fig. 7. Variation of selectivity to acrylic acid with propene conversion during various testing cycles: **CT5**$^{(350)}$ (●); **CT6**$^{(400)}$ (▲); **CT7**$^{(400)}$ (○); **HCT**$^{(400)}$ (■). For comparison, the selectivity achieved at 300 °C during the **CT4**$^{(300)}$ experiment is also included (▲). (For interpretation of the references to color in this figure legend, the reader is referred to the web version of the article.)

Fig. 5 shows the influence of the catalyst pre-treatment with moisture and of the presence of water in the reaction mixture on the propene conversion in **CT** runs of **C**-series. The conversion on the catalyst pre-treated with humid oxygen in **CT7**$^{(400)}$ run progressively increases with temperature up to 400 °C. Nevertheless, the highest conversion (30–35%) was obtained in **HCT**$^{(400)}$ run working with traces of water in the feed at 380 °C, decreasing at higher temperatures (Fig. 5). The catalytic data shown in Fig. 5 indicate that, as previously reported [5], the presence of humidity in the feed considerably increases the effectiveness of the catalytic surface. The improved activity is obtained in the temperature range 350–400 °C and is supported by the conductivity results presented in Figs. 2 and 4 demonstrating that the lattice mobilization takes place in this temperature range. Thus, reduction by propene and possibly by its partial oxidation products in **CT** runs or re-oxidation by oxygen occurs more efficiently between 350 and 400 °C. At low temperatures, water seems to compete with oxygen for adsorption on anion vacancies, as shown previously for other oxides [28], while chemisorbed water moderates the extensive surface oxidation at high temperatures especially when water is fed with the reaction mixture.

Fig. 7 shows the variation of the selectivity to acrylic acid with propene conversion in experiments of **B**- and **C**-series. Maximum selectivity to acrylic acid has been obtained in **HCT**$^{(400)}$ run, in which water was included in the feed. Nevertheless, the selectivity was improved when the catalytic test was performed on the catalyst re-oxidated at 400 °C and especially when re-oxidation was carried out in an humid atmosphere. These results are in agreement with those previously reported on MoVTeNbO catalysts in which the presence of water in the feed has a strong influence on the selectivity to acrylic acid [38].

4. General remarks

The *operando* measurements of the electrical conductivity of MoVTeNb-M2 phase submitted to different treatments allowed to get valuable information on the importance of the oxidation level of the catalyst surface during propene oxidation. As mentioned in Section 1 the primary goal of this study was only to follow the phenomenological aspects and not to obtain absolute values of conductivity/activity. The most important conclusions reached are summarized below.

The electrical conductivity results obtained in **A**-series (without any treatment with oxygen between successive catalytic tests) showed that advanced surface reduction occurs on heating above 350 °C under reaction conditions.

At this moment, it is difficult to evaluate the extent of surface reduction on the basis of these transient measurements. This would need stationary state, kinetic measurements, at various temperatures, which obviously involve changing the sample after each catalytic test (with the risk of introducing errors related to the homogeneity of the sample). The scope of this study was to heat the sample over the whole temperature range under different atmospheres, in order to identify some temperature domains/reaction conditions significant for the catalyst operation. Surface reduction detected by conductivity measurements in the catalytic test mixture containing also oxygen is indicative for the fact that, at least above 350 °C, surface reduction by propene (and by its reaction products, having also a reductive action) prevails, re-oxidation being slower. This can occur also as a result of the variation of the propene/oxygen ratio along the catalyst bed. However, since the reported activity trend is based on the effluent analysis simultaneously measured with conductivity, we believe that the association of these activity data with changes of the reduction/oxidation levels (based on the response of the electrical conductivity) is relevant.

Thus, the general behaviour of the sample depends on the maximum heating temperature; 350 °C seems to be a critical temperature for the onset of lattice mobilization, associated with either advanced reduction (under catalytic reaction,) or surface oxidation (under oxygen flow).

Since MoVTeNbO-M2 phase seems to be rather stable up to 350 °C under oxygen and under reaction conditions (in **B**-series) it can be stated that up to this temperature reduction or oxidation is probably limited to the surface over-layer only. In this respect, the sample behaves as proposed by Guliants et al. [22], namely the bulk oxide can be considered as a support of the surface layer, which is more susceptible to interact with the reactants. It is obvious that depending on the temperature, bulk defects will be also involved in the reaction by controlling the oxidation level of the surface. However, by taking into account the above presented data, this is not expected to occur below 350 °C. The results also prove the reversibility of the level of surface reduction/oxidation, an important fact for exploiting the catalyst in practice. However, we must note that since the catalytic tests were relatively short, we cannot anticipate the effect of surface over-reduction for long-term catalyst operation.

Water is only weakly adsorbed at low temperature on the oxidized surface (see **HO**$^{(400)}$ run). However, a reduced surface resulting from high temperature catalytic testing, seems to be much more sensitive to moisture adsorption (see the comments on the effluent content in **DHe4**$^{(400)}$ and in next cycles and also see the plot **HCT**$^{(400)}$ cycle). The presence of water in the reaction feed prevents coke formation but also extensive surface re-oxidation. It can be supposed that water is preferentially adsorbed on anionic vacancies; this blocks the oxygen access to the surface and prevents its re-oxidation, unless a high temperature treatment (above 350 °C), induces water desorption/surface oxidation (see **DO3**). At this moment, further investigations are required to establish if water species adsorbed at low temperatures remain molecular or partly dissociate to form surface OH groups.

Finally, the evolution of the conversion/selectivity in comparison with the initial tests suggests the necessity of preventing over-reduction using a slightly higher content of oxygen in the feed just from the beginning, as previously suggested [17]. At the same time, it seems that the role of water could be to moderate the surface oxidation.

Acknowledgment

T.B. and J.M.L.N thank for the financial support from DGICYT in Spain through Project CTQ2006-09358/BQU).

References

[1] T. Ushikubo, K. Oshima, A. Kayo, T. Umezawa, K. Kiyono, I. Sawaki, EP Patent 0,529,853 A2 (1992); assigned to Mitsubishi.
[2] T. Ushikubo, K. Oshima, A. Kayou, M. Hatano, Stud. Surf. Sci. Catal. 112 (1997) 473.
[3] T. Ushikubo, H. Nakamura, Y. Koyasu, S. Wajiki, US Patent 5,380,933 (1995); assigned to Mitsubishi.
[4] J.M. López Nieto, P. Botella, M.I. Vázquez, A. Dejoz, Chem. Commun. (2002) 1906.
[5] P. Botella, E. García-González, J.M. López Nieto, M.I. Vázquez, J. González-Calbet, J. Catal. 225 (2004) 428.
[6] H. Tsuji, Y. Koyasu, J. Am. Chem. Soc. 124 (2002) 5608.
[7] J.M.M. Millet, H. Roussel, A. Pigamo, J.L. Dubois, J.C. Jumas, Appl. Catal. A 232 (2002) 77.
[8] P. Botella, J.M. López Nieto, B. Solsona, A. Mifsud, F. Márquez, J. Catal. 209 (2002) 445.
[9] D. Vitry, Y. Morikawa, J.L. Dubois, W. Ueda, Appl. Catal. A 251 (2003) 411.
[10] R.K. Grasselli, J.D. Burrington, D.J. Buttrey, P. DeSanto Jr., C.G. Lugmair, A.F. Volpe, T. Weingand, Top. Catal. 23 (2003) 5.
[11] E. García-González, J.M. López Nieto, P. Botella, J.M. González-Calbet, Chem. Mater. 14 (2002) 4416.
[12] E. García-González, J.M. López Nieto, P. Botella, B. Solsona, J.M. González-Calbet, Mater. Res. Soc. Symp. Proc. 755 (2003) 327.
[13] P. DeSanto Jr., D. Buttrey, R.K. Grasselli, C.G. Lugmair, A.F. Volpe, B.H. Toby, T. Vogt, Z. Kristallogr. 219 (2004) 152.
[14] M. Lundberg, M. Sundberg, Ultramicoscopy 52 (1993) 429.
[15] A. Magnelli, Acta Chem. Scand. 7 (1953) 315.
[16] M. Baca, M. Aouine, J.L. Dubois, J.M.M. Millet, J. Catal. 233 (2005) 234.
[17] J. Holmberg, R.K. Grasselli, A. Andersson, Appl. Catal. A 270 (2004) 121.
[18] P. Botella, J.M. López Nieto, B. Solsona, Catal. Lett. 78 (2002) 383.
[19] J. Holmberg, R.K. Grasselli, A. Andersson, Top. Catal. 23 (2003) 55.
[20] J. Holmberg, S. Hansen, R.K. Grasselli, A. Andersson, Top. Catal. 38 (2006) 17.
[21] K. Asakura, K. Nakatani, T. Kubota, Y. Iwasawa, J. Catal. 194 (2000) 309.
[22] V.A. Guliants, R. Bhandari, H.H. Brongersma, A. Knoester, A.M. Gaffney, S. Han, J. Phys. Chem. B 109 (2005) 10234.
[23] (a) C.G. Koops, Phys. Rev. 83 (1951) 121;
(b) C.M. Huggins, A.H. Sharbaugh, J. Chem. Phys. 38 (1963) 391.
[24] J.F. McAleer, P.T. Moseley, J.O.W. Norris, D.E. Williams, J. Chem. Soc., Faraday Trans. I 83 (1987) 1323.
[25] S.R. Morrisson, The Chemical Physics of Surfaces, 2nd ed., Plenum Press, 1990, p. 69 (Chapter 5).
[26] D.C. Hill, H.L. Tuller, Ceramic sensors: theory and practice, in: R.C. Buchanan (Ed.), Ceramic Materials for Electronics, Processing, Properties and Applications, Marcel Dekker Inc, NY, 1991, p. 249 (Chapter 5).
[27] M. Caldararu, D. Sprinceana, N.I. Ionescu, Ber. Bunsenges. Phys. Chem. 97 (1993) 369.
[28] M. Caldararu, D. Sprinceana, V.T. Popa, N.I. Ionescu, Sens. Actuators B30 (1996) 35.
[29] M. Caldararu, G. Postole, C. Hornoiu, V. Bratan, M. Dragan, N.I. Ionescu, Appl. Surf. Sci. 181 (2001) 255.
[30] M. Caldararu, G. Postole, M. Carata, M. Chelu, C. Hornoiu, N.I. Ionescu, T. Jouchakova, A. Redey, Appl. Surf. Sci. 211 (2003) 156.
[31] J.J. Fripiat, A. Jelli, G. Poncelet, J. Andre, J. Phys. Chem. 69 (1965) 2185.
[32] A. Bielanski, M. Najbar, M. Simonska Stachura, Bull. Acad. Pol. Sci., Ser. Sci. Chim. 26 (1978) 249.
[33] A. Bielanski, M. Najbar, Z. Zientarski, Bull. Acad. Pol. Sci. Ser. Sci. Chim. 27 (1979) 417.
[34] M. Najbar, K. Stadnicka, J. Chem. Soc., Faraday Trans. I. 79 (1983).
[35] M. Caldararu, Thesis, Center of Physical Chemistry Bucharest, 1983.
[36] K.D. Kreuer, Th. Dippel, N.G. Haynovsky, J. Maier, Ber. Bunsengens. Phys. Chem. 96 (1992) 1736.
[37] P. Colomban, A. Novak, in: P. Colomban (Ed.), Proton Conductors, Cambridge University Press, Cambridge, 1992, p. 38 (Chapter 3).
[38] J.M. Oliver, J.M. López Nieto, P. Botella, Catal. Today 96 (2004) 241.